

Preprint PFC/JA-84-31

GENERATION OF ELECTROMAGNETIC RADIATION FROM A ROTATING
ELECTRON RING IN A RIPPLED MAGNETIC FIELD

Y.Z. Yin and G. Bekefi

Plasma Fusion Center and
Research Laboratory of Electronics
Massachusetts Institute of Technology
Cambridge, MA. 02139

August 1984

GENERATION OF ELECTROMAGNETIC RADIATION FROM A ROTATING
ELECTRON RING IN A RIPPLED MAGNETIC FIELD

Y.Z. Yin* and G. Bekefi

Department of Physics and Research Laboratory of Electronics

Massachusetts Institute of Technology

Cambridge, Massachusetts 02139

ABSTRACT

Calculations show that modes resembling the free electron laser (FEL) instability are excited when electrons move in quasi-circular orbits under the combined action of a uniform axial magnetic field and an azimuthally periodic wiggler magnetic field. In the model, a thin annular ring of rotating electrons is confined in a hollow cylindrical waveguide, or between concentric cylinders comprising a coaxial waveguide, and the dispersion equations for the transverse magnetic ($TM_{\ell m}$) modes are derived and analyzed. Coherent radiation occurs near frequencies ω corresponding to the crossing points of the electromagnetic modes $\omega = \omega_c(\ell, m)$ and the beam modes $\omega = (\ell + N)\Omega_{II}$, where ω_c and Ω_{II} are the waveguide cutoff frequency and the electron cyclotron frequency, respectively, and N is the number of wiggler periods. The computed instability growth rates are found to be somewhat larger than those calculated for the conventional, linear FEL.

*Permanent address: Institute of Electronics, Academia Sinica, Beijing, Peoples's Republic of China.

I. INTRODUCTION

Numerous theoretical¹ and experimental² studies have been carried out of free-electron lasers (FEL's) in linear geometry with spatially periodic transverse^{1,2} or longitudinal³⁻⁶ magnetic wiggler fields. Such configurations have gain limitations imposed by the finite length of the interaction region. Recently, a novel circular version of the free-electron laser has been explored both theoretically⁷⁻⁹ and experimentally^{10,11} in which a rotating, relativistic electron stream is subjected to an azimuthally periodic wiggler field. The potential advantages of circular FEL's as compared with the conventional linear form are several. First, the beam circulates continuously through the wiggler field resulting in a long effective interaction region. Secondly, because of the recirculation of the growing electromagnetic wave, the device provides its own internal feedback and is in essence an oscillator rather than an amplifier, as is the case in linear FEL's. And thirdly, because the electron motion is primarily circular the system¹⁰ is very compact.

There are several ways of producing a rotating relativistic electron stream. One is to subject the electrons to orthogonal electric and magnetic fields as is typical in magnetron-like devices. Here, the electrons undergo a $\vec{v}(r) = \vec{E}_o(r) \times \vec{B}_|| / |\vec{B}_|||^2$ drift in a radial electric field $\hat{r}E_o(r)$ and a uniform axial magnetic field $\hat{z}B_||$. Addition of an azimuthally periodic magnetic field $\vec{B}_w(\theta, r)$ then results in a circular FEL. This scheme has been explored previously,^{7,8,10} and though the experimental results¹⁰ are encouraging, it may have a potential drawback in that the electron velocity $v(r)$ varies strongly with radial distance r . This velocity shear leads to certain complications,¹² and may also cause a reduction in gain and efficiency of the device.

Employing an entirely different scheme, experiments have been recently described¹¹ which generate an essentially monoenergetic rotating electron ring, thereby circumventing the problem of velocity shear mentioned above. There,

an annular, nonrotating beam propagating axially is injected into a narrow magnetic cusp which transforms^{13,14} the axial beam energy into rotational energy. The integrity of the annular ring of rotating electrons is maintained downstream from the cusp by a uniform axial guide magnetic field.

Superimposed on the axial guiding magnetic field is an azimuthally periodic magnetic wiggler field \vec{B}_w , which, near the center of the gap, is primarily¹⁰ radial and is thus transverse to the electron flow velocity, as is the case in conventional linear free-electron lasers. The wiggler field is generated by an assembly of samarium cobalt bar magnets placed behind two concentric metal cylinders. Thus, the electrons see only smooth metallic boundaries which act as the coaxial waveguide for the radiation. The proximity of the metallic walls to the electron ring also helps to stabilize^{15,16} the negative mass instability, the excitation of which is often a worrisome problem.¹⁷

The purpose of this paper is to examine the microwave generation process caused by relativistically rotating electrons moving in quasi-circular orbits under the combined action of a uniform axial magnetic field and an azimuthally periodic wiggler magnetic field, as discussed above. Section II contains a description of the configuration, and an analysis of the beam dynamics. Section III contains the derivation of the dispersion relations for the transverse magnetic ($TM_{\ell m}$) modes excited by the electron ring confined in cylindrical or coaxial waveguide systems. In Section IV we present examples of computer generated solutions of the dispersion equations, and finally Section V contains a discussion of the results.

We will show that growing electromagnetic fields occur near frequencies corresponding to the crossing points of the $TM_{\ell m}$ waveguide modes, $\omega = \omega_c(\ell, m)$, and the beam modes $\omega = (\ell + N)\Omega_{\parallel}$, where ω_c is the waveguide cutoff frequency, Ω_{\parallel} is the electron cyclotron frequency, and N is the number of wiggler periods around the circumference.

II. ELECTRON MOTION IN THE GUIDE AND WIGGLER FIELDS

In our model, an annular electron ring of infinite axial extent and very small thickness rotates within a cylindrical waveguide of radius a , or within the gap formed by two concentric grounded metal cylinders of radii a and b , as is illustrated in Fig. 1. The two cylinders form a coaxial waveguide. The electron ring is confined by a uniform axial magnetic field $B_{\parallel}\hat{z}$ directed along the waveguide axis. The electrons are assumed to have zero streaming velocity, and in the absence of any other perturbations, they undergo pure rotation about the z axis with an azimuthal velocity

$$v_{\theta}^{(o)} = r_o \Omega_{\parallel}. \quad (1)$$

Here r_o is the radius of the electron ring and $\Omega_{\parallel} = eB_{\parallel}/\gamma_o m_o c$ is the electron cyclotron frequency in the guide field; $\gamma_o = (1 - \beta_{\theta_o}^2)^{-\frac{1}{2}} = 1 + eV/m_o c^2$ is the relativistic energy factor, $\beta_{\theta_o} = v_{\theta}^{(o)}/c$ and eV is the beam kinetic energy.

Superimposed on the axial magnetic field $B_{\parallel}\hat{z}$, is an azimuthally periodic wiggler field \vec{B}_w (Fig. 1) which perturbs the electron stream. Subject to the requirement that $\nabla \cdot \vec{B}_w = \nabla \times \vec{B}_w = 0$, the field in the vacuum gap between the concentric cylinders a, b is calculated to be,¹⁰

$$\begin{aligned} \vec{B}_w = & \hat{r} \frac{B_{ow}}{2} \cos(N\theta) \left[\left(\frac{r}{a} \right)^{N-1} + \left(\frac{b}{r} \right)^{N+1} \right] \left[\frac{a}{b} \right]^{(N^2-1)/2N} \\ & - \hat{\theta} \frac{B_{ow}}{2} \sin(N\theta) \left[\left(\frac{r}{a} \right)^{N-1} - \left(\frac{b}{r} \right)^{N+1} \right] \left[\frac{a}{b} \right]^{(N^2-1)/2N} \end{aligned} \quad (2)$$

where \hat{r} and $\hat{\theta}$ are unit vectors in the radial and azimuthal directions, respectively. $N = \pi(a+b)/\lambda_o$ is the number of spatial periods and λ_o is the linear periodicity defined midway in the gap. B_{ow} is the amplitude of the radial component of field at a distance $r = R_o \equiv (a^{N-1} b^{N+1})^{1/(2N)}$ where the azimuthal field component vanishes (which is roughly midway between the electrodes). We see that

near the center of the gap the wiggler field is primarily radial and is thus transverse to the electron flow velocity, as is the case in conventional free electron lasers. The undulatory force $-e\frac{\vec{v}}{c} \times \vec{B}_W$ is along the $\pm z$ axis. We shall find in section III that this undulatory motion gives rise to a z-directed RF current which excites growing transverse magnetic ($TM_{\ell m}$) waveguides modes.

To simplify computations we shall assume henceforth that the electron ring radius r_o coincides exactly (or nearly so) with the radius $R_o \equiv (a^{N-1} b^{N+1})^{1/2N}$ discussed above. Under these conditions the $\hat{\theta}$ component of \vec{B}_W can be neglected, and \vec{B}_W of Eq. (2) becomes

$$\vec{B}_W = \hat{r} B_{oW} \cos(N\theta) \quad (3)$$

We shall now assume a sufficiently weak pump field such that,

$$f \equiv |\Omega_W / N\Omega_{||}| \ll 1. \quad (4)$$

Here $\Omega_W = eB_{oW} / m_o c \gamma_o$ is the cyclotron frequency associated with the wiggler field and $\Omega_{||} = eB_{||} / m_o c \gamma_o$ is the cyclotron frequency associated with the axial, guide field. Subject to this inequality the motion of the electrons in the absence of RF fields is given by

$$\left. \begin{aligned} v_r^{(o)} &= 0 \\ v_\theta^{(o)} &= r_o \dot{\theta}^{(o)} = r_o \Omega_{||} \\ v_z^{(o)} &= c \beta_{\theta o} f \sin(N\Omega_{||} t) \end{aligned} \right\} \quad (5)$$

and,

$$\left. \begin{aligned} r^{(o)} &= r_o \\ \theta^{(o)} &= \Omega_{||} t \\ z^{(o)} &= \frac{1}{N} r_o f [1 - \cos(N\Omega_{||} t)] \end{aligned} \right\} \quad (6)$$

where,

$$\beta_{\theta o} = v_\theta^{(o)} / c ; \gamma_o = (1 - \beta_{\theta o}^2)^{-\frac{1}{2}} .$$

We note that inequality (4) does not restrict the wiggler strength excessively. Since in most practical consideration $N \gg 1$, B_w and $B_{||}$ can have approximately equal magnitudes. In deriving the equations of motion, the self-fields of the electron ring are neglected under the present assumption of a tenuous beam.

In the presence of electromagnetic fields, the equation of motion of an electron is given by

$$\frac{d\vec{v}}{dt} = -\frac{e}{m_o \gamma} \left[\vec{E} + \frac{1}{c} \vec{v} \times \vec{B} - \frac{1}{c^2} (\vec{v} \cdot \vec{E}) \vec{v} \right] \quad (7)$$

where $\vec{v} = \vec{v}^{(0)} + \vec{v}^{(1)}$, $\vec{E} = \vec{E}^{(1)}$, $\vec{B} = \vec{B}_{||}^{(0)} + \vec{B}_w^{(0)} + \vec{B}^{(1)}$, etc. are sums of zero-order quantities described by superscripts "o" and small, time-dependent, RF quantities denoted by superscripts "1". Linearizing Eq. (7) then leads to

$$\begin{aligned} \ddot{r}^{(1)} - c\beta_{\theta 0} \gamma_o^2 \dot{\theta}^{(1)} - \beta_{\theta 0}^2 \Omega_{||}^2 \gamma_o^2 r^{(1)} - \gamma_o^2 \beta_{\theta 0}^2 f \Omega_{||} \sin(N\theta) \dot{z}^{(1)} \\ = -\frac{e}{m_o \gamma_o} \left[E_r^{(1)} + \beta_{\theta 0} B_z^{(1)} - \beta_{\theta 0} f \sin(N\theta) B_{\theta}^{(1)} \right] ; \\ r_o \ddot{\theta}^{(1)} + \Omega_{||} \dot{r}^{(1)} + N \Omega_{||} f \cos(N\theta) \dot{z}^{(1)} = -\frac{e}{m_o \gamma_o} \left[\frac{E_{\theta}^{(1)}}{\gamma_o^2} + \beta_{\theta 0} f \sin(N\theta) B_r^{(1)} - \beta_{\theta 0}^2 f \sin(N\theta) E_z^{(1)} \right] ; \\ \ddot{z}^{(1)} + \gamma_o^2 \beta_{\theta 0}^2 \Omega_{||}^2 N f \cos(N\theta) r^{(1)} + c\beta_{\theta 0} N f (\gamma_o^2 \beta_{\theta 0}^2 - 1) \cos(N\theta) \dot{\theta}^{(1)} \\ = -\frac{e}{m_o \gamma_o} \left[E_z^{(1)} - \beta_{\theta 0} B_r^{(1)} - \beta_{\theta 0}^2 f \sin(N\theta) E_{\theta}^{(1)} \right] , \end{aligned} \quad (8)$$

where we have used

$$\frac{1}{\gamma} = \frac{1}{\gamma_o} \left[1 - \frac{\gamma_o^2 (\vec{v}^{(0)} \cdot \vec{v}^{(1)})}{c^2} \right]$$

These results will be used in deriving the dispersion equations in Section III below.

III. DISPERSION RELATIONS

In the case of a tenuous electron ring being considered here, the coaxial waveguide modes can be approximated in form by the unperturbed, vacuum, trans-

verse electric (TE) and transverse magnetic (TM) modes. The z-directed oscillatory motion given by Eqs. (5) and (6) caused by the wiggler field does not couple to the TE family of modes, and they are therefore of no further interest (the negative mass instability and the synchronous mode instability,¹⁸ which do couple to TE modes are assumed to be stabilized by the proximity of the cylinder walls). The dispersion equation for the remaining TM family of modes is computed under cutoff conditions corresponding to the case for which the axial wavenumber $k_{||}=0$. Since the electrons have no axial streaming velocity, $k_{||}=0$ corresponds to the case where the growth rate of the FEL instability is expected to be largest. The RF fields are then given by

$$\begin{aligned} E_z^{(1)} &= \sum_{\ell=-\infty}^{+\infty} C_{\ell} X_{\ell}(k_c r) e^{i(\ell\theta - \omega t)} \\ B_r^{(1)} &= \sum_{\ell=-\infty}^{+\infty} C_{\ell} \frac{1}{k_c^2} \ell \frac{\omega}{c} \frac{1}{r} X_{\ell}(k_c r) e^{i(\ell\theta - \omega t)} \\ B_{\theta}^{(1)} &= \sum_{\ell=-\infty}^{+\infty} i C_{\ell} \frac{1}{k_c} \frac{\omega}{c} X'_{\ell}(k_c r) e^{i(\ell\theta - \omega t)} \end{aligned} \quad (9)$$

with $E_r^{(1)} = E_{\theta}^{(1)} = B_z^{(1)} = 0$. In the above equation C_{ℓ} is a constant proportional to the perturbing TM field,

$$X_{\ell}(k_c r) = J_{\ell}(k_c r) N_{\ell}(k_c a) - J_{\ell}(k_c a) N_{\ell}(k_c r) \quad (10)$$

and J_{ℓ} and N_{ℓ} are Bessel functions of the first and second kind, respectively; $k_c(\ell, m)$ is the cutoff wave number determined by setting $X_{\ell}(k_c b) = 0$. The cutoff frequency ω_c of the (ℓ, m) th wave-guide mode is related to the wave number $k_c(\ell, m)$ through $\omega_c(\ell, m) = ck_c(\ell, m)$; ℓ and m are the azimuthal and radial mode numbers, respectively.

All components of the TM fields in the coaxial waveguide can now be found from the wave equation for the axial electric field, namely

$$(\omega^2 - c^2 k_c^2) E_z^{(1)} = -i 4\pi \omega J_z^{(1)} \quad (11)$$

The RF current density of the infinitely thin ring at $r=r_0$ is¹⁸

$$J_z^{(1)} = \sigma_0 \delta(r-r_0) v_z^{(1)} - \sigma_0 \delta'(r-r_0) r^{(1)} v_z^{(0)} + \sigma^{(1)} \delta(r-r_0) v_z^{(0)} \quad (12)$$

where

$$\begin{aligned} \sigma_0 & \text{ is unperturbed surface charge density, } \sigma^{(1)} \text{ is perturbed density,} \\ \sigma^{(1)} & = -\sigma_0 \left(\frac{r^{(1)}}{r} + \frac{\partial \theta^{(1)}}{\partial \theta} \right) \quad , \end{aligned} \quad (13)$$

and δ is the Dirac delta function.

To obtain the dispersion equations, we expand all first order, time varying quantities (such as $r^{(1)}$, $\theta^{(1)}$, $v_z^{(1)}$, $E_z^{(1)}$ etc.) in the form

$$F = \sum_{\ell=-\infty}^{+\infty} \tilde{F}_\ell e^{i(\ell\theta - \omega t)} \quad (14)$$

and eliminate RF terms between Eqs. (8), (11) and (12). After some tedious algebra one obtains the following dispersion equation for the (complex) radiation frequency:

$$\left[\omega^2 - c^2 k_c^2 - \frac{1}{4} \omega_p^2 \frac{r_0^2}{D_\ell} \frac{\omega}{\Omega_\ell} \left(\frac{\ell \omega}{k_c^2 r_0 c} \beta_{\theta 0} - 1 \right) \chi_\ell^2(k_c r_0) \right] \left[\Delta_{\ell+N} \right] = \frac{1}{4} \omega_p^2 \frac{r_0^2}{D_\ell} f_{\Omega_\ell \omega T} \quad (15)$$

Here

$$\omega_p = \left(4\pi e \sigma_0 / m_0 \gamma_0 r_0 \right)^{\frac{1}{2}} \quad (16)$$

is the electron plasma frequency,

$$\Delta_\ell = \Omega_\ell^2 \left[\Omega_\ell^2 - \Omega_{\parallel}^2 - \frac{\psi_\ell \Omega_{\parallel}^2}{1 + \psi_\ell (\beta_{\theta 0}^2 \gamma_0^2 - 1)} \right] \left[1 + \psi_\ell (\beta_{\theta 0}^2 \gamma_0^2 - 1) \right] \quad (17)$$

$$D_\ell = \left[\frac{r^2}{2} \left\{ N_\ell^{-2}(k_c a) \left[J_\ell^{-2}(k_c r) + \left(1 - \frac{\ell^2}{k_c^2 r^2} \right) J_\ell^2(k_c r) \right] + J_\ell^{-2}(k_c a) \left[N_\ell^{-2}(k_c r) + \left(1 - \frac{\ell^2}{k_c^2 r^2} \right) N_\ell^2(k_c r) \right] \right. \right.$$

$$\left. \left. - 2N_\ell^{-1}(k_c a) J_\ell^{-1}(k_c a) \left[J_\ell^{-1}(k_c r) N_\ell^{-1}(k_c r) + \left(1 - \frac{\ell^2}{k_c^2 r^2} \right) J_\ell(k_c r) N_\ell(k_c r) \right] \right\} \right]_{r=b}^{r=a}$$

$$\begin{aligned}
 T = & \xi_{1\ell} + N X_{\ell} (k_c r_o) X'_{\ell} (k_c r_o) \left[\beta_{\theta o} f \frac{\omega}{k_c c} b_1 + 2\beta_{\theta o}^2 \gamma_o^2 f \Omega_{\parallel} k_c r_o \frac{1}{\Omega_{\ell}} b_3 \right] \\
 & + \eta_{2\ell} + N X_{\ell} (k_c r_o) X'_{\ell} (k_c r_o) \beta_{\theta o} f \frac{\omega}{k_c c} b_2 \\
 & - \xi_{2\ell} + N X_{\ell}^2 (k_c r_o) \left[\beta_{\theta o} \gamma_o^2 f b_1 b_4 + \gamma_o^2 \frac{\Omega_{\ell} \omega}{\Omega_{\ell}} b_1 b_3 + \beta_{\theta o}^2 \gamma_o^2 f - \gamma_o^2 \frac{\Omega_{\ell} \omega}{\Omega_{\ell}} \right] \\
 & - \eta_{1\ell} + N X_{\ell}^2 (k_c r_o) \left[\beta_{\theta o} f b_2 b_4 + \frac{\Omega_{\ell} \omega}{\Omega_{\ell}} b_2 b_3 \right] \\
 & - \xi_{1\ell} + N X_{\ell}^2 (k_c r_o) \left[\beta_{\theta o}^2 \gamma_o^2 f \Omega_{\parallel} \frac{1}{\Omega_{\ell}} b_1 b_3 - \beta_{\theta o} f \frac{\omega r_o}{c} \left(1 - \frac{\ell^2}{k_c^2 r_o^2} \right) - \beta_{\theta o}^2 \gamma_o^2 f \Omega_{\parallel} \frac{1}{\Omega_{\ell}} \right] \\
 & - \eta_{2\ell} + N X_{\ell}^2 (k_c r_o) \beta_{\theta o}^2 \gamma_o^2 f \Omega_{\parallel} \frac{1}{\Omega_{\ell}} b_2 b_3 \\
 & - \xi_{1\ell} + N X_{\ell}^{-2} (k_c r_o) \beta_{\theta o} f \frac{\omega r_o}{c} \\
 & + \xi_{2\ell} + N X_{\ell} (k_c r_o) X'_{\ell} (k_c r_o) \left[2\beta_{\theta o} \gamma_o^2 f k_c r_o b_4 + 2\gamma_o^2 k_c r_o \frac{\Omega_{\ell} \omega}{\Omega_{\ell}} b_3 \right]
 \end{aligned}$$

$$b_1 = 1 + \beta_{\theta o}^2 \gamma_o^2 N \Omega_{\parallel} \frac{1}{\Omega_{\ell}}$$

$$b_2 = (\ell + N) - \beta_{\theta o}^2 \gamma_o^2 N \frac{\Omega_{\ell} + N}{\Omega_{\ell}}$$

$$b_3 = 1 - \beta_{\theta o} \frac{\ell \omega}{k_c^2 r_o c}$$

$$b_4 = \frac{\ell \omega}{k_c^2 r_o c} - \beta_{\theta o}$$

$$\Omega_{\ell} = \omega - \ell \Omega_{\parallel}$$

$$\psi_{\ell} = \frac{1}{2} \frac{\Omega_{\ell}^2}{\Omega_{\ell} - N \Omega_{\ell} + N}$$

$$\xi_{1\ell} = \left[1 + \frac{1}{2} \Omega_{\ell}^2 (\beta_{\theta o}^2 \gamma_o^2 - 1) \frac{1}{\Omega_{\ell} - N \Omega_{\ell} + N} \right] \Omega_{\ell}^2$$

$$\xi_{2\ell} = \left[1 + \frac{1}{2} \beta_{\theta 0}^2 \Omega_{\omega}^2 (\beta_{\theta 0}^2 \gamma_0^2 - 1) \frac{1}{\Omega_{\ell-N} \Omega_{\ell+N}} \right] \Omega_{\parallel} \Omega_{\ell}$$

$$\eta_{1\ell} = \Omega_{\ell}^2 + \beta_{\theta 0}^2 \gamma_0^2 \Omega_{\parallel}^2 \left(1 + \frac{1}{2} \beta_{\theta 0}^2 \gamma_0^2 \Omega_{\omega}^2 \frac{1}{\Omega_{\ell-N} \Omega_{\ell+N}} \right)$$

$$\eta_{2\ell} = \left[1 + \frac{1}{2} \beta_{\theta 0}^2 \gamma_0^2 \Omega_{\omega}^2 \frac{1}{\Omega_{\ell-N} \Omega_{\ell+N}} \right] \Omega_{\parallel} \Omega_{\ell}$$

Despite the complexity of dispersion Eq. (15), its physical structure is readily understood. The left-hand side describes the interacting waves; the right-hand side is the coupling term which vanishes when the amplitude of the wiggler field B_w goes to zero. To examine the structure of the waves we set the right side equal to zero. Then the first term on the left-hand side in the square brackets represents the (ℓ, m) th electromagnetic perturbation under cutoff conditions ($k_{\parallel}=0$). When ω_p is small, it reduces to

$$\begin{aligned} \omega &= ck_c(\ell, m) \\ \text{or} \quad \omega &= \omega_c(\ell, m) . \end{aligned} \tag{18}$$

The second term in square brackets given by $\Delta_{\ell+N}$ represents one of two beam modes. The first mode

$$\begin{aligned} \Omega_{\ell+N} &= 0 \\ \text{or} \quad \omega &= (\ell+N) \Omega_{\parallel} \end{aligned} \tag{19}$$

is a "synchronous mode"¹⁸ upshifted in frequency by the wiggler periodicity N . The second mode is a "cyclotron" mode¹⁸

$$\begin{aligned} \Omega_{\ell+N}^2 &= \Omega_{\parallel}^2 \\ \text{or} \quad \omega &= (\ell+N \pm 1) \Omega_{\parallel} \end{aligned} \tag{20}$$

likewise upshifted by N .

The interaction of the electromagnetic wave (18) with the cyclotron mode

(20) proves to be stable, and is of no further interest here. However, the interaction between the electromagnetic mode (18) and synchronous mode (19) is unstable and represents the sought-after instability. The maximum growth rate occurs close to the crossing points of

$$\omega = \omega_c(\ell, m) \quad (21)$$

and

$$\omega = (\ell + N)\Omega_{\parallel} \quad (22)$$

The radiation frequencies ω are then determined when these two equations are satisfied simultaneously.

We may now define $k_{\theta} = \ell/r$ as the azimuthal propagation constant of the RF perturbation, and $k_w = N/r$ as the wiggler wave constant (r is the radius). Since $\Omega_{\parallel} = v_{\theta}^{(0)}/r$, (Eq. (1)), Eq. (22) can be cast into the form

$$\omega = (k_{\theta} + k_w)v_{\theta}^{(0)} \quad (23)$$

which is the familiar expression for the propagation of the ponderomotive wave in a free electron laser. Combining Eq. (24) with Eq. (21) yields the following alternate expression for the radiation frequency:

$$\begin{aligned} \omega &= \frac{N\Omega_{\parallel}}{1 - (\ell\Omega_{\parallel}/\omega_c(\ell, m))} \\ &= \frac{k_w v_{\theta}^{(0)}}{1 - (v_{\theta}^{(0)}/v_{p\theta})} \end{aligned} \quad (24)$$

where $v_{p\theta} = \omega_c(\ell, m)r/\ell (> c)$ is the azimuthal phase velocity of the RF perturbation. Equation (24) is to be compared with $\omega = (k_w v_o)/(1 - v_o/c)$ for the conventional free electron laser in its normal linear geometry with v_o as the axial electron velocity.

It is clear from Eqs. (21) and (22) that for a given wiggler periodicity N , high frequency radiation arises from coupling to high waveguide mode numbers. We note that when the gap width $(a-b)$ is sufficiently small so that

$(a-b)/a \ll 1$, ω_c is to fair approximation given by,¹⁹

$$\omega_c(\ell, m) \approx \pi m c / (a-b) \quad (25)$$

provided that m is not too small. This shows that the cutoff frequencies of the TM coaxial waveguide modes are governed primarily by the radial wavenumbers m . On the other hand, the frequencies of the beam wave (Eq. (22)) are governed by the azimuthal wave numbers ℓ . However, we shall see in Section IV that the situation is different for a hollow cylindrical waveguide.

IV. NUMERICAL EXAMPLES

For relativistic electrons, $(\beta_{\theta 0} \gamma_0)^2 \gg 1$, dispersion Eq. (15) simplifies somewhat with the result that

$$\left[\omega^2 - c^2 k_c^2 - \frac{1}{4} \omega_p^2 \frac{r_0^2}{D_\ell} \frac{\omega}{N \Omega_{\parallel}} \left(\frac{\ell \omega}{k_c^2 r_0 c} \beta_{\theta 0} - 1 \right) X_\ell^2(k_c r_0) \right] \left[\omega - (\ell + N) \Omega_{\parallel} \right]^2 = \frac{1}{4} \omega_p^2 \frac{r_0^2}{D_\ell} \beta_{\theta 0}^2 f^2 \omega_{\Omega_{\parallel}} (\ell + N) X_\ell^2(k_c r_0) \quad (26)$$

The examples that follow were obtained by solving this equation on a computer for complex frequencies ω .

Case (a): $m=1$

Here we consider relatively low frequencies in which coupling occurs with the $TM_{\ell 1}$ mode of a coaxial waveguide with $a=6\text{cm}$ and $b=5\text{cm}$. The radius of the electron ring $r_0=R_0=5.42\text{cm}$ is at a position where the wiggler magnetic field is purely radial (Eq. (2)). The nonrelativistic plasma frequency $\omega_{p0} = \omega_p \gamma_0^{\frac{1}{2}} = 1.50 \times 10^9 \text{sec}^{-1}$; $B_{\parallel} = 1.52\text{kG}$; $B_w = 1.21\text{kG}$ and $N=8$; $\gamma_0 = 4.91$.

Figure 2a shows the crossing points between the $TM_{\ell 1}$ mode and the beam wave $\omega = (\ell + N) \Omega_{\parallel}$. Two crossings occur, one for the azimuthal wavenumber $\ell=16$ and the other for the wavenumber $\ell=21$. For these values of ℓ the insta-

bility growth rates are expected to be maximum. This is borne out by calculations of the imaginary part of the frequency, ω_i , shown plotted in Fig. 2b. Note, that although solid lines have been drawn, physically meaningful growth rates occur only at integer values of ℓ . The growth rate is maximum when parameters are adjusted in such a way that the two crossing points coalesce at $\ell \approx 18$.

Figures 3a and 3b illustrate the dependence of the instability growth rate ω_i on the strength of the wiggler magnetic field, and on the electron plasma frequency ω_p , respectively. We find that $\omega_i \propto B_W^2/3$, and $\omega_i \propto \omega_p^2/3$ which is just as one would expect¹ for the case of a cold but tenuous beam in the "single particle, high gain, strong pump" regime of FEL operation.

Case (b): m=5-12

Here we consider relatively high frequencies in which coupling occurs with $TM_{\ell m}$ modes having large wave numbers ℓ and m . This situation is more akin to recent experiments.¹¹ The outer and inner waveguide radii are $a=6.58\text{cm}$, $b=5.25\text{cm}$; $r_o=R_o=5.77\text{cm}$; the nonrelativistic plasma frequency $\omega_{po} \equiv \omega_p \gamma_o^{\frac{1}{2}} = 1.50 \times 10^9 \text{sec}^{-1}$; $B_{||}=1.25\text{kG}$; $B_W=0.75\text{kG}$ and $N=6$; $\gamma_o=4.35$.

Figure 4a gives a plot of the maximum growth rate ω_i as a function of the real part of the frequency ω_r for six successive modes ranging from $m=5$ to $m=10$. The apparently strange behavior seen in the figure, in which ω_i exhibits an initial rapid decrease with m followed by a subsequent increase, is readily explained. The electron ring is infinitely thin and has a fixed radius $r=r_o=R_o$ for all m . However, as m changes the RF electric field, amplitude at $r=r_o$ goes through maxima and minima depending on the value of m . This strongly affects the coupling of the RF fields to the beam and thus affects the growth rate. Figure 4b shows how $E_z(r=r_o)$ varies with ω_r . We see that the growth rate of Fig. 4a mimicks the electric field behavior of Fig. 4b.

In a realistic situation the annular electron ring has finite thickness

and thus the electrons "sample" a range of RF fields at various radii r . The best that can be achieved is to place a thin ring at an electric field anti-mode. We therefore calculated the maximum growth rates for various ring radii $r=r_0$ (near $r=R_0$) ranging from 5.67cm to 6.27cm. In doing this we kept $B_{||}$ and B_w fixed but allowed γ_0 to vary in accordance with the constraint imposed by Eq. (1). The results of these calculations are illustrated in Fig. 5 where each point corresponds to a different value of r_0 . We see in contrast with Fig. 4a, that now the maximum growth rates of successive radial modes m are nearly equal in magnitude.

Case (c): $m=1, b=0$ (no inner electrode).

We have seen in Sections IV(a) and (b) that for a coaxial waveguide with $(a-b)/a \ll 1$ the cutoff frequencies $\omega_c(\ell, m)$ for the TM modes we are almost independent of the azimuthal wave number ℓ (Eq. (26)). Thus, in order to achieve high frequency radiation and satisfy the mandatory coupling of Eqs. (21) and (22), it is necessary to go to high radial mode numbers m (see Fig. 5). Matters are quite different when the inner electrode is removed. Now, the cutoff frequency ω_c increases quickly with increasing ℓ , and high frequencies are readily achieved even for small m ($m=1$, for example).

In the case of a hollow cylindrical waveguide, $X_\ell(k_c r)$ of Eq. (10) becomes

$$X_\ell(k_c r) = J_\ell(k_c r) \quad (27)$$

and the cutoff wavenumber and frequency are determined by $J_\ell(k_c a) = 0$. For $m=1$ and large azimuthal wave numbers²⁰ one obtains to good approximation,

$$\begin{aligned} \omega_c(\ell, 1) &= ck_c(\ell, 1) \\ &= (c/a)F(\ell) \\ &= (c/a) \left(\ell + 1.85575\ell^{1/3} + 1.03315\ell^{-1/3} + \dots \right) . \end{aligned} \quad (28)$$

We can now substitute Eq. (28) in Eq. (21) and obtain ℓ corresponding to the

crossing points with Eq. (22). To find ℓ for the maximum growth rate of the instability, the two curves represented by Eqs. (21) and (22) must meet tangentially, with the result that

$$(N+\ell) \frac{dF(\ell)}{d\ell} = F(\ell) \quad (29)$$

where the dimensionless function $F(\ell)$ is defined in Eq. (28). Thus, we see that the value of the azimuthal wave number ℓ (for $\ell \gg 1$), corresponding to the maximum growth rate, depends only on the number of wiggler periods N . For example, when $N=6$, $\ell=107$.

Once ℓ is found from Eq. (29), the remaining parameters of the system are then fully determined. With $\ell=107$, and $a=6.58\text{cm}$, Eqs. (21) and (28) yield $\omega=\omega_c=5.2800 \times 10^{11} \text{rad. sec}^{-1}$, and from Eq. (22) it follows that $\Omega_{\parallel}=4.6814 \times 10^9 \text{rad. sec}^{-1}$. Since the electron ring radius $r_o=R_o=5.77\text{cm}$, one finds from Eq. (1) that $v_{\theta}^{(o)}/c=0.90039$, $\gamma=2.2984$ and $B_{\parallel}=0.610\text{kG}$. A conventional, linear FEL with the same parameters and also operating at the tangential intersection of the relevant waves would radiate at a frequency $\omega=1.48 \times 10^{11} \text{rad. sec}^{-1}$.

Of course, the growth rate of the instability must be obtained by solving the complete dispersion equation. The equation for an electron ring in a hollow waveguide of radius a is the same as that given by Eq. (26), except that now X_{ℓ} is given by (27) and D_{ℓ} is given by

$$D_{\ell} = \frac{a^2}{2} \left[J_{\ell}^{\prime 2}(k_c a) + \left[1 - \frac{\ell^2}{k_c^2 a^2} \right] J_{\ell}^2(k_c a) \right] \quad (30)$$

Using the above parameters together with $\omega_{p0}=\omega_p \gamma_o^{1/2}=1.5 \times 10^9 \text{sec}^{-1}$ and $B_w=0.75\text{kG}$ yields $\omega_i=9.83 \times 10^8 \text{rad. sec}^{-1}$.

Calculations similar to the above were carried out for several different values of wiggler periodicity N , with $a=6.58\text{cm}$, $r_o=5.77\text{cm}$, and $B_w=0.75\text{kG}$. The results are presented in Table I. We see that extremely high radiation frequencies ω can be achieved at relatively low beam energies simply by a moder-

ate increase in the wiggler periodicity N . The reason is that for large azimuthal wave numbers ℓ , solution of Eq. (29) gives

$$\ell \approx 0.529N^3 \quad (31)$$

from which we see that a two-fold increase in N (for example) result in an ~ 8 fold increase in the radiation frequency. We note that this behavior is quite different from a conventional free electron laser operating in linear geometry where the radiation frequency scales linearly with the wiggler periodicity.

The growth rates ω_i shown in Table I are seen to vary rapidly with N . The reason is similar to the rapid changes in ω_i illustrated in Fig. 4. Namely, the electron ring radius r_o is held at a fixed value which is not necessarily optimum for good coupling with E_z , the RF electric field. As discussed earlier in connection with Fig. 5, optimization of ω_i can be achieved by slight variations of r_o . We have taken 7 discrete values of r_o in the range from 5.67cm to 6.27cm. Table II gives the largest values of ω_i calculated in that range. We see that now ω_i is relatively insensitive to the value of N , whereas the beam energy is strongly dependent on N (and r_o).

V. DISCUSSION

In this paper we have derived conditions under which growing electromagnetic waves can be excited by a rotating, relativistic electron ring subjected to an azimuthally periodic wiggler magnetic field. The thin, tenuous electron ring undergoes pure rotation (the axial velocity is zero) and is comprised of an assembly of monoenergetic electrons with zero energy spread. The rotational motion $v_\theta^{(o)} = \Omega_{||} r_o$ is perturbed by a radially directed, azimuthally periodic wiggler magnetic field, as a result of which growing electromagnetic modes are excited. The excitation frequencies and temporal growth rates are derived for the $TM_{\ell,m}$ family of modes that can be supported in a hollow cylindrical waveguide of radius a , or an coaxial waveguide with radii a and b . The appropriate

dispersion equations are derived for complex frequencies ω under the assumption that the axial wave vector k_{\parallel} of the electromagnetic fields is zero (cutoff condition). It is found that radiation growth occurs near frequencies corresponding to the crossing points of the cutoff waveguide modes $\omega = \omega_c(\ell, m)$ (ω_c is the cutoff frequency) and the beam modes $\omega = (\ell + N)\Omega_{\parallel}$ (Ω_{\parallel} is the electron cyclotron frequency) upshifted by the wiggler periodicity N . This coupling is similar in nature to that which occurs in conventional, linear free electron lasers. The computed instability growth rates are found to be somewhat larger than those for the liner FEL's under the same conditions (same γ , B_w , ω_p , etc). Coupling to high $T_{\ell 1}$ modes of a hollow cylindrical waveguide reveals that very short wavelengths in the millimeter wavelength range can be achieved with relatively low beam energies of several hundred kilovolts, and weak magnetic fields of approximately half a kilogauss. To achieve similar frequencies, the gyrotron²¹ would require magnetic fields about two orders in magnitude higher.

ACKNOWLEDGEMENTS

This work was supported by the U.S. Department of Energy (Cont. DE-FG05-84ER13272).

REFERENCES

1. N.M. Kroll and W. A. McMullin, Phys. Rev. A17, 300 (1978); P. Sprangle and R.A. Smith, Phys. Rev. A21, 293 (1980) and references therein.
2. P.A. Sprangle, R.A. Smith, and V.L. Granatstein, in Infrared and Sub-millimeter Waves, edited by K. Button (Academic, New York, 1979), Vol. 1, p. 279 and references therein.
3. W.A. McMullin and G. Bekefi, Appl. Phys. Lett. 39, 845 (1981).
4. W.A. McMullin and G. Bekefi, Phys. Rev. A25, 1826 (1982).
5. R.C. Davidson and W.A. McMullin, Phys. Rev. A26, 1997 (1982).
6. R.C. Davidson and W.A. McMullin, Phys. Fluids 26, 840 (1983).
7. G. Bekefi, Appl. Phys. Lett. 40, 578 (1982).
8. R.C. Davidson, W.A. McMullin, and K. Tsang, Phys. Fluids, 27, 233 (1984).
9. C-L. Chang, E. Ott, T.M. Antonsen, Jr. and A.T. Drobot, SAI Report No. SAI-83-1214 (1983).
10. G. Bekefi, R.E. Shefer, and B.D. Nevins, Massachusetts Institute of Technology, Cambridge, Massachusetts, Plasma Fusion Center Report No. PFC/JA-83-3, 1983; also Lasers '82, Society for Optical and Quantum Electronics, SOQUE, 1982 (STS, 1982), p. 136.
11. G. Bekefi, R.E. Shefer, and W.W. Destler, Appl. Phys. Lett. 44, 280 (1984).
12. F.V. Hartemann, R.E. Shefer, and G. Bekefi, Proc. 1984 IEEE Inter. Conf. Plasma Science, St. Louis, Missouri, 1984 p. 97.
13. M.J. Rhee and W.W. Destler, Phys. Fluids 17, 1574 (1974).
14. W.W. Destler, P.K. Misra, and M.J. Rhee, Phys. Fluids 18, 1820 (1975).
15. R.J. Briggs and V.K. Neil, Plasma Physics 9, 209 (1962).
16. L.J. Laslett, IEEE Trans. Nucl. Sci. NS-20, 271 (1973).
17. Y.Y. Lau and D. Chernin, Phys. Rev. Lett. 52, 1425 (1984).
18. P. Sprangle, J. Appl. Phys. 47, 2935 (1976).

19. N. Marcuvitz, "Waveguide Handbook" (Boston Technical Publishers 1964)
p. 74. Our mode designation (ℓ, m) should not be confused with the (m, n)
designation of the reference.
20. M. Abramowitz and A. Stegun "Handbook of Mathematical Functions" (Nat'l.
Bureau of Standards 1964)p. 371.
21. P. Sprangle and A.T. Drobot, IEEE Trans. Microwave Theory Tech. 25, 528
(1977).

TABLE I. Computed parameters for an electron ring of fixed radius $r_o = 5.77\text{cm}$ rotating in a hollow cylindrical waveguide of radius $a = 6.58\text{cm}$; $\omega_{p0} = 1.5 \times 10^9 \text{rad. sec}^{-1}$; $B_w = 0.75\text{kG}$.

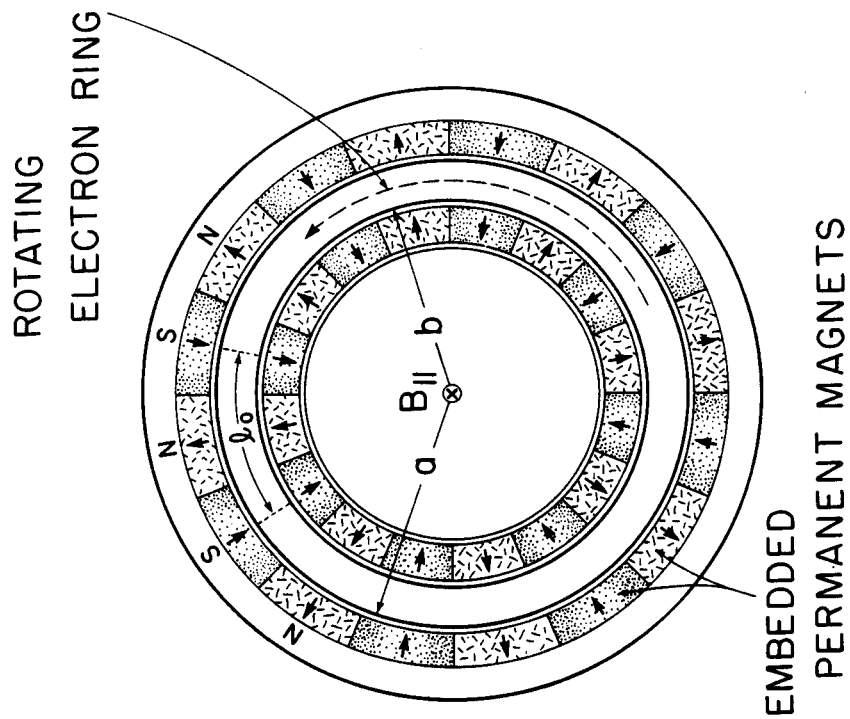
N	ℓ	V(MV)	$B_{ }$ (kG)	$\omega_r \times 10^{-11} (\text{rad. sec}^{-1})$	$\omega_i \times 10^{-7} (\text{rad. sec}^{-1})$
4	29	0.884	0.752	1.59	162
6	107	0.660	0.610	5.28	98.3
8	261	0.607	0.576	12.4	4.34
10	516	0.585	0.562	24.2	2.55
12	898	0.574	0.554	41.7	50.8

TABLE II. Optimized growth rate parameters for electron rings of various radii rotating in a cylindrical waveguide of radius $a = 6.58\text{cm}$; $\omega_{p0} = 1.5 \times 10^9 \text{rad. sec}^{-1}$; $B_w = 0.75\text{kG}$.

N	ℓ	r_o (cm)	V(MV)	$B_{ }$ (kG)	$\omega_r \times 10^{-11} (\text{rad. sec}^{-1})$	$\omega_i \times 10^{-9} (\text{rad. sec}^{-1})$
4	29	5.71	0.807	0.710	1.59	1.70
6	107	6.07	1.08	0.827	5.28	1.87
8	261	6.30	1.62	1.10	12.4	1.49
10	516	6.31	1.53	1.05	24.2	1.26
12	898	5.72	0.545	0.539	41.5	39.0

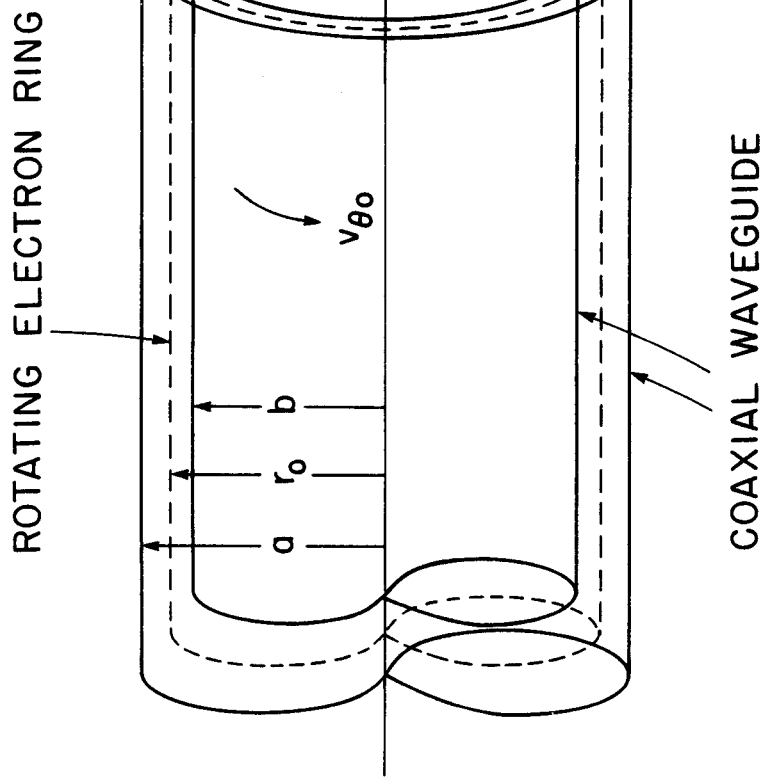
FIGURE CAPTIONS

- Fig. 1. Schematic drawing of a rotating electron ring in a radially directed, azimuthally periodic wiggler magnetic field.
- Fig. 2. (a) Coupling of the $TM_{\ell,1}$ coaxial waveguide modes with the beam modes as a function of the azimuthal wave number ℓ ; (b) growth rate of the FEL instability as a function of ℓ . $a=6\text{cm}$, $b=5\text{cm}$; $r_o=5.42\text{cm}$; $\omega_{p0} = 1.50 \times 10^9 \text{rad. sec}^{-1}$; $N=8$; $\gamma_o=4.91$; $B_{||}=1.52\text{kG}$; $B_w=1.21\text{kG}$.
- Fig. 3. Variation of the instability growth rate as a function of (a) wiggler field amplitude, (b) electron plasma frequency. $a=6\text{cm}$, $b=5\text{cm}$; $r_o=5.42\text{cm}$; $n=8$; $\gamma_o=4.91$; $B_{||}=1.52\text{kG}$.
- Fig. 4. (a) Growth rates of the $TM_{\ell,5}$ to $TM_{\ell,10}$ coaxial waveguide modes and (b) amplitude of the RF electric field at fixed radius $r_o=R_o=5.77\text{cm}$, as a function of the radiation frequency. $a=6.58\text{cm}$; $b=5.25\text{cm}$; $\omega_{p0} = 1.50 \times 10^9 \text{rad. sec}^{-1}$; $N=6$; $\gamma_o=4.35$; $B_{||}=1.25\text{kG}$; $B_w=0.75\text{kG}$.
- Fig. 5. Growth rates of the $TM_{\ell,5}$ to $TM_{\ell,10}$ coaxial waveguide modes for 7 different electron ring radii r_o ranging from 5.67cm to 6.27cm. Each point is for a different value of r_o . The open circles are for the case $r_o=R_o=5.77\text{cm}$ and correspond to the points shown in Fig. 4. $a=6.58\text{cm}$; $b=5.25\text{cm}$; $\omega_{p0} = 1.5 \times 10^9 \text{rad. sec}^{-1}$; $N=6$; $B_{||}=1.25\text{kG}$; $B_w=0.75\text{kG}$.



ROTATING
ELECTRON RING

EMBEDDED
PERMANENT MAGNETS



ROTATING ELECTRON RING

COAXIAL WAVEGUIDE

Fig. 1
Yin & Bekefi

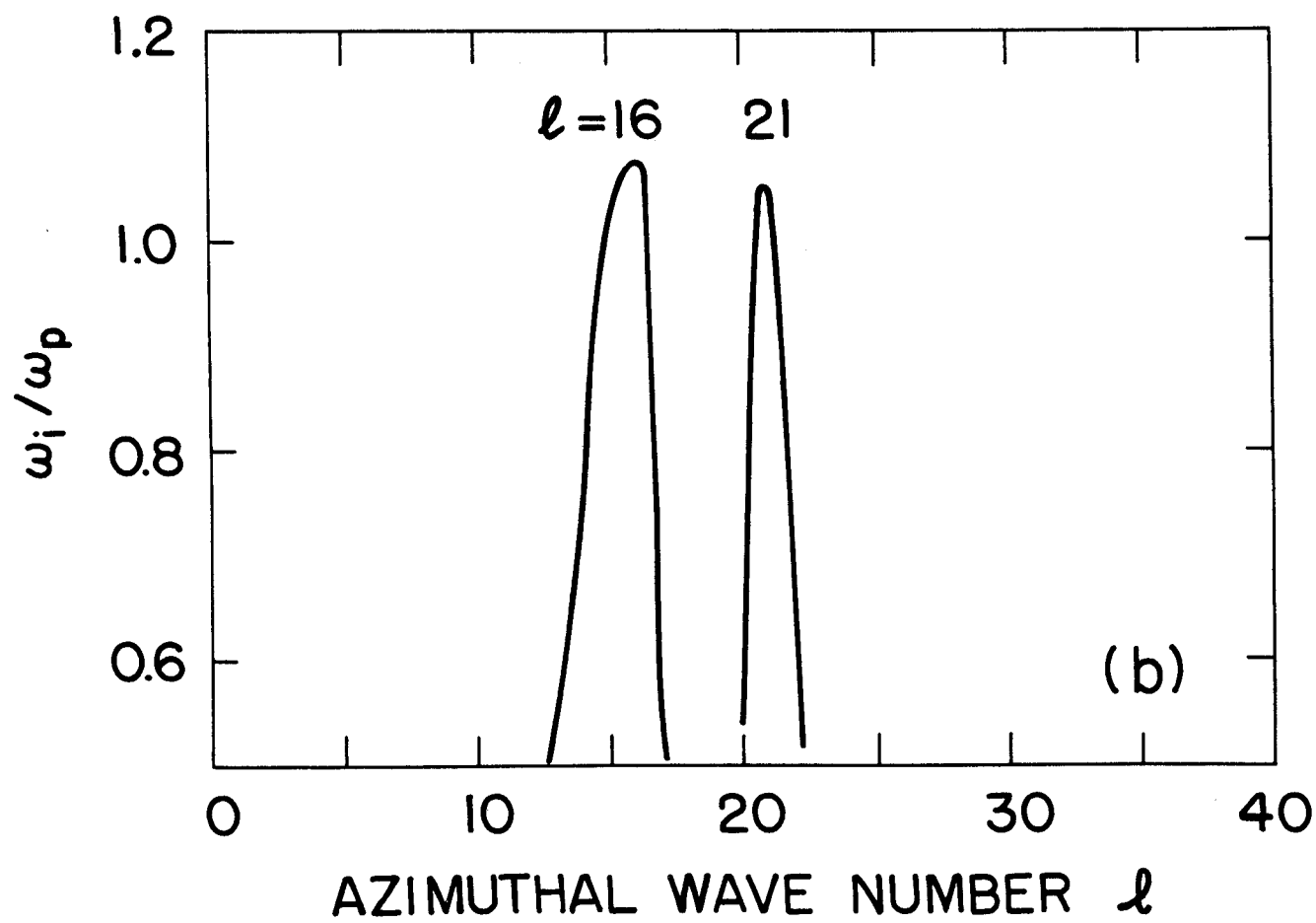
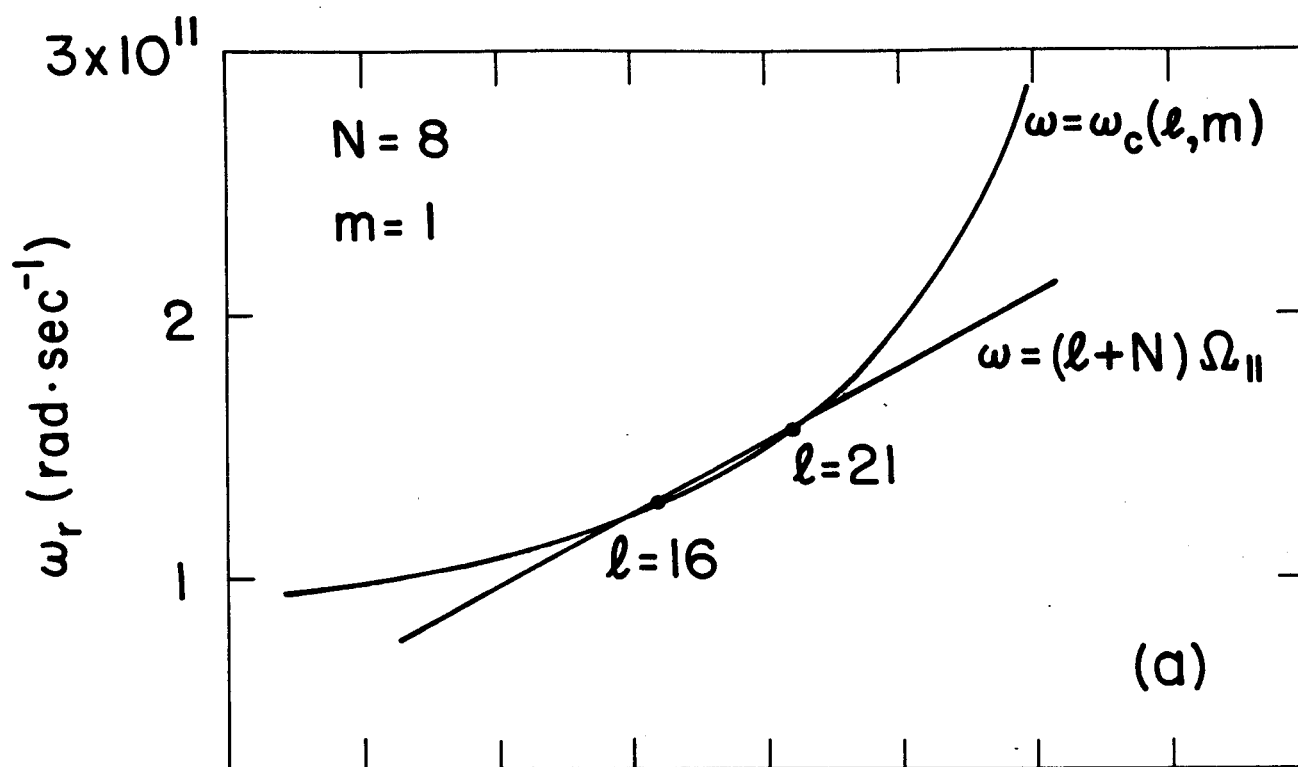


Fig. 2
Yin & Bekefi

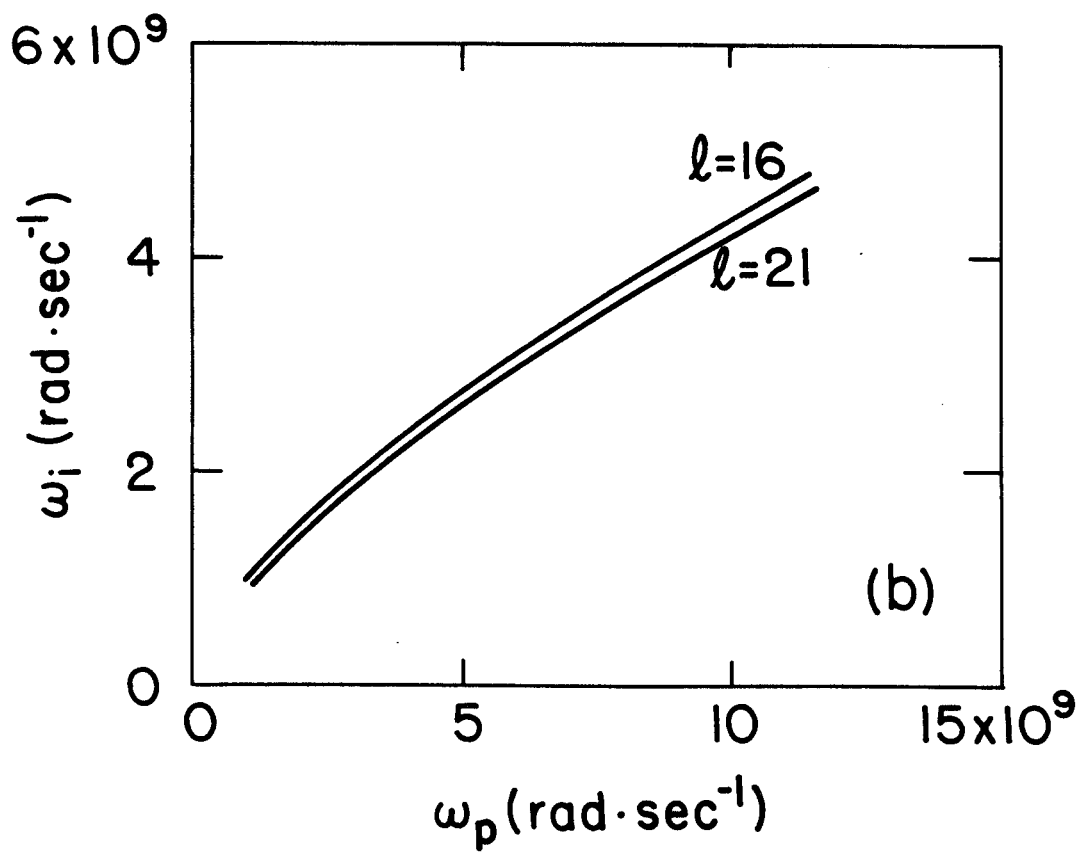
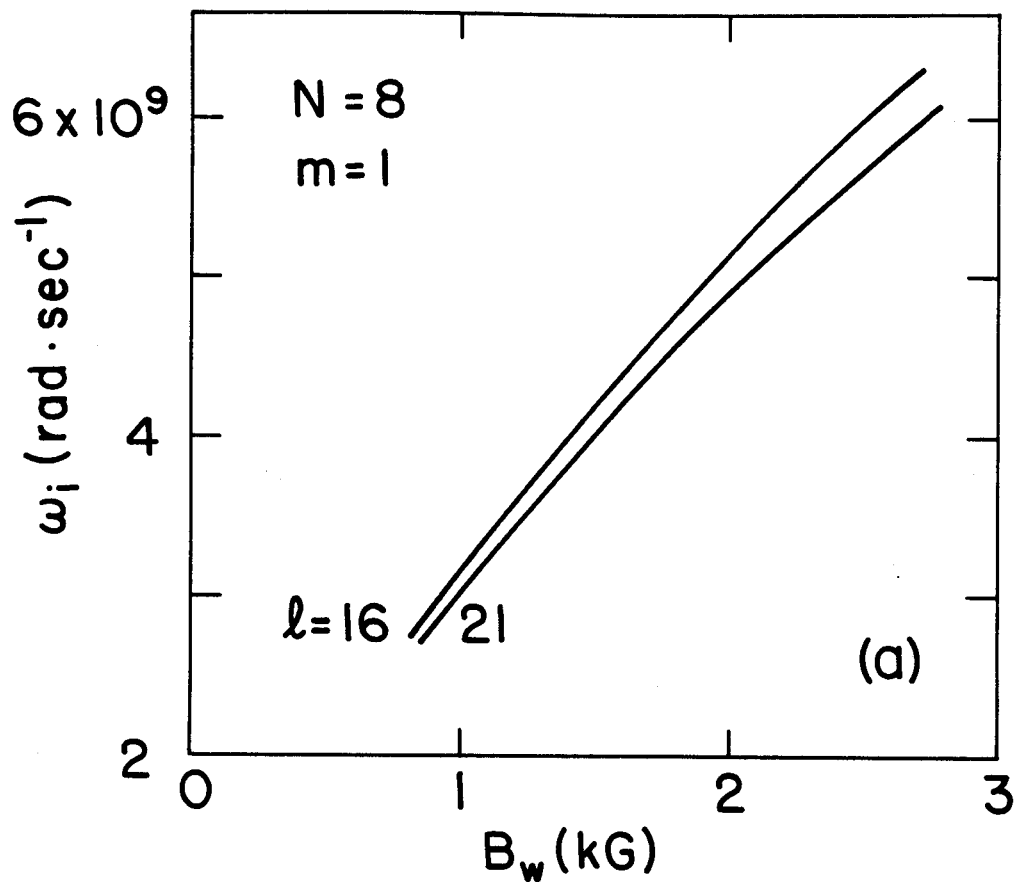


Fig. 3
Yin & Bekefi

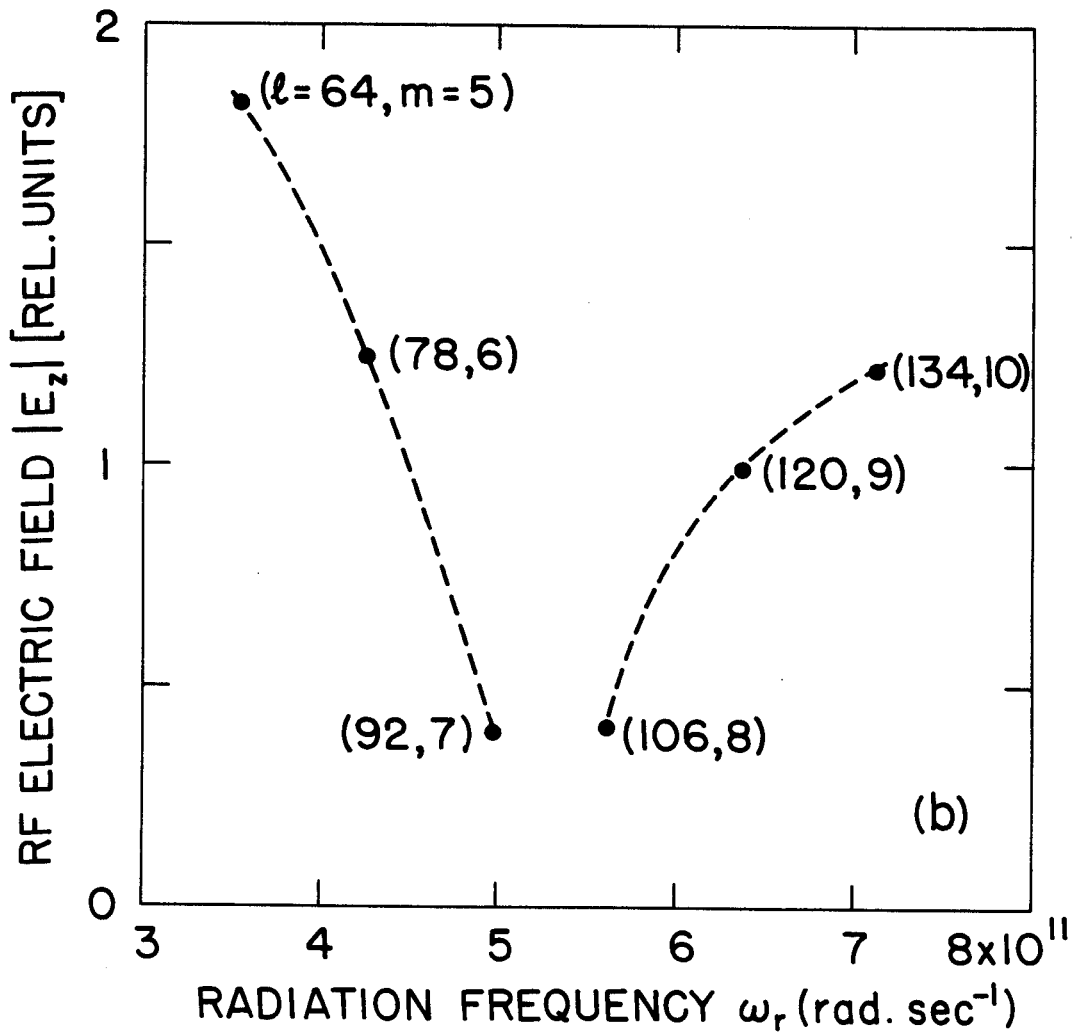
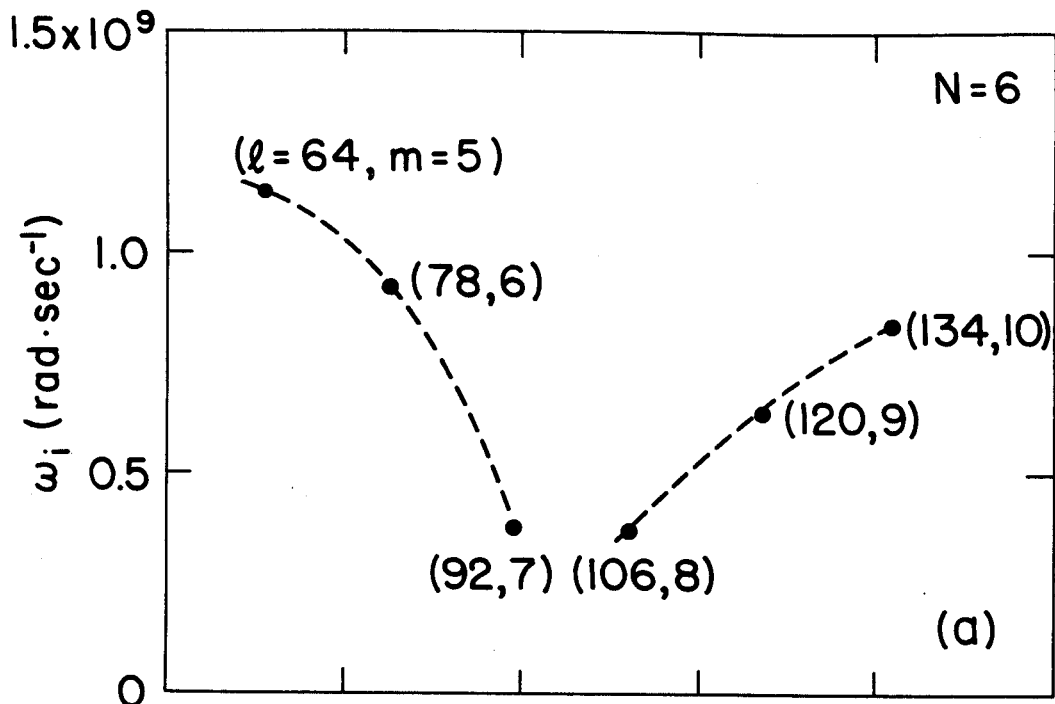


Fig. 4
Yin & Bekefi

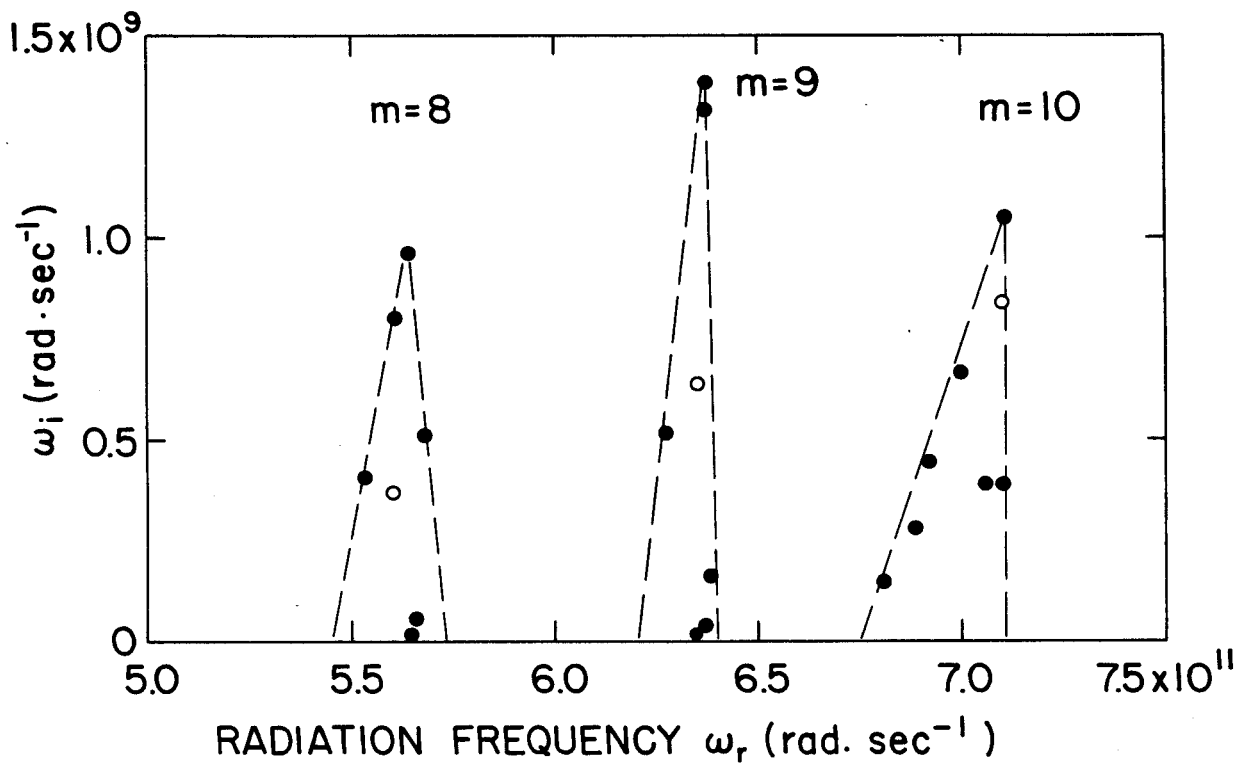
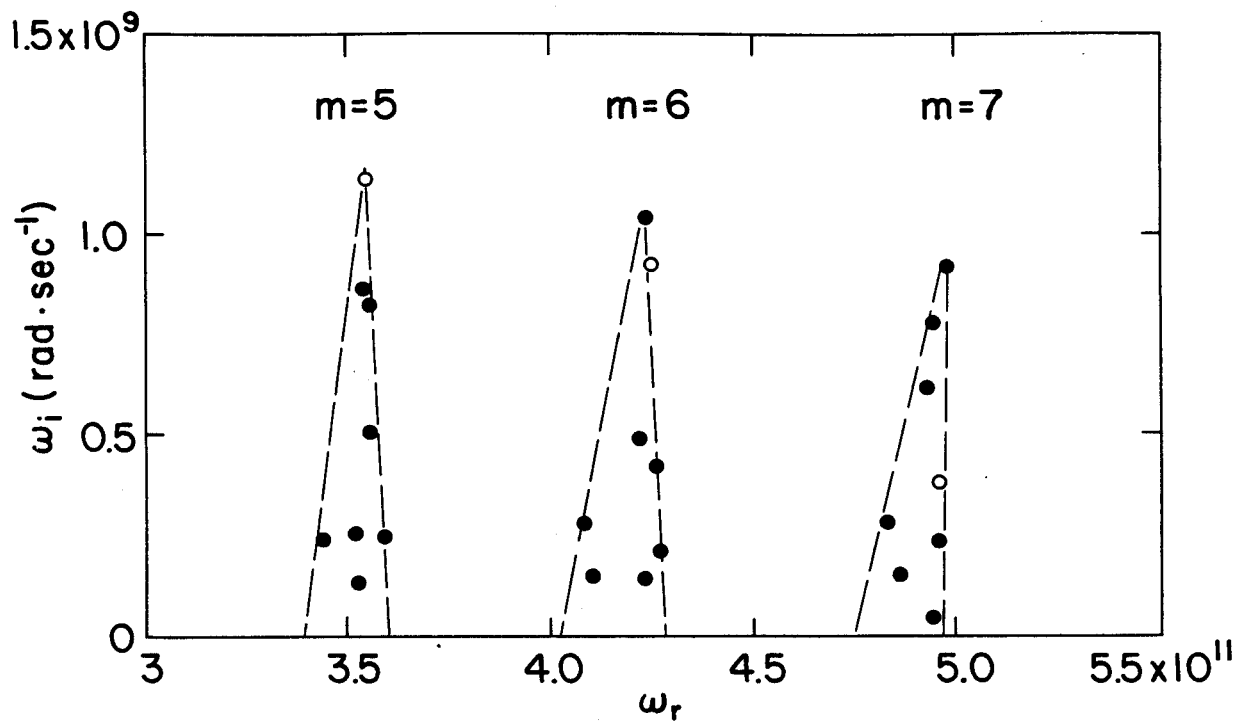


Fig. 5
Yin & Bekefi